Electronic supplementary information *for*

n-Type Conjugated Polymers Based on 3,3′-Dicyano-2,2′-Bithiophene: Synthesis and Semiconducting Properties

Ying Sui,[a] Yunfeng Deng,*[a] Yang Han,[a] Jidong Zhang,[c] Wenping Hu[b] and Yanhou Geng*[ab]

[a]School of Materials Science and Engineering, Tianjin University, Tianjin 300072, P. R. China.

[b]Tianjin Key Laboratory of Molecular Optoelectronic Science, Tianjin University, and Collaborative Innovation Center of Chemical Science and Engineering (Tianjin), Tianjin 300072, P. R. China.

[c]State Key Laboratory of Polymer Physics and Chemistry, Changchun Institute of Applied Chemistry, Chinese Academy of Sciences, Changchun 130022, P. R. China.

*E-mail: yunfeng.deng@tju.edu.cn; yanhou.geng@tju.edu.cn

General methods

^{1}H NMR and ^{13}C NMR spectra were recorded using a Bruker 400-MHz spectrometer in chloroform-d ($CDCl_3$) or 1,1,2,2-tetrachloroethane-d$_2$ ($C_2D_2Cl_4$) at 25 °C or 120 °C with tetramethylsilane (TMS) as internal reference. Elemental analysis was conducted on a FlashEA1112 elemental analyzer. Matrix-assisted laser desorption ionization time-of-flight (MALDI-TOF) mass spectra were measured by a Bruker/AutoflexIII Smartbean MALDI mass spectrometer with

2-[(2E)-3-(4-t-buthylphenyl)-2-methylprop-2-enylidene]malononitrile (DCTB) as the matrix in a reflection mode. High temperature gel permeation chromatography (HT-GPC) analysis of the polymers was performed on a PL-GPC 220 system with 1,2,4-trichlorobenzene as the eluent and polystyrene as the standard at 150 $^{\mathrm{o}}$C. Thermogravimetric analysis (TGA) was carried out on a TA Q50 thermogravimetric analyzer with the heating rate of 10 $^{\mathrm{o}}$C min^{-1} at a nitrogen flow. Differential scanning calorimetry (DSC) was conducted on a TA Q2000 instrument with a heating/cooling rate of 10 $^{\mathrm{o}}$C min^{-1} under nitrogen. UV-vis-NIR absorption spectra were obtained on a Shimadzu UV3600-plus spectrometer. Solution spectra were measured in 1,2-dichlorobenzene (*o*-DCB) with a concentration of 1×10^{-5} mol L^{-1} and films were prepared by spin-casting with *o*-DCB as solvent. The optical bandgap was calculated according to absorption onset of films ($E_{\mathrm{g}}^{\mathrm{opt}} = 1240/\lambda_{\mathrm{onset}}$ eV). Film cyclic voltammetry (CV) test was carried out on a CHI660a electrochemical analyzer with a three electrode cell at a scan rate of 100 mV s^{-1} in anhydrous acetonitrile with tetrabutylammonium hexafluorophosphate (Bu_4NPF_6, 0.1 mol L^{-1}) as the supporting electrolyte. A glassy carbon electrode with a diameter of 10 mm, a Pt wire, and a saturated calomel electrode (SCE) were used as the working, counter, and reference electrodes, respectively. Density functional theory (DFT) calculations were conducted by Gaussian 09 with a hybrid B3LYP correlation functional and 6-31G (d) basis set and the 4-decyltetradecyl side chain was simplified as methyl group. The two-dimensional grazing incidence wide angle X-ray scattering (2D GIWAXS) was measured at Shanghai Synchrotron Radiation Facility (SSRF) on beam line BL14B1

(λ = 0.124 nm) with a MarCCD area detector at incidence angle of 0.2°. In plane and out of plane GIWAXS of the thin films were measured by a Rigaku Smart Lab with Cu K_α source (λ = 1.54056 Å) in air. Atomic force microscopy (AFM) measurements were performed in tapping mode on a Bruker MultiMode 8 instrument. The thicknesses of spin-cast films were measured by AFM (Bruker MultiMode 8 instrument) and those of drop-cast films were measured by Stylus Profiler (Bruker DektakXT instrument)

Fabrication and characterization of organic thin film transistors (OTFTs)

The charge transport properties of the polymers were characterized by using top gate and bottom contact (TGBC) OTFTs. Highly n-doped silicon wafers covered with a 300 nm thick thermally grown SiO_2 layer, which are commercially available and have flat and smooth surface, were used as substrates. The substrates were washed by an ultrasonic cleaner with deionized water, acetone and isopropanol, dried under a nitrogen flow and heated at 120 °C for 10 min. Au (30 nm) was deposited on the silicon substrate as source and drain electrodes with W/L = 70 (W = 5600 μm, L = 80 μm). The polymer films (~20 nm) were spin coated from *o*-DCB solutions with a concentration of 4.0 mg mL^{-1} at 1000 rpm. Then the films were annealed at 100, 150, 200 or 250 °C for 10 min. Then the dielectric layer (~600 nm) was spin coated atop from butyl acetate solution (80 mg mL^{-1}) of poly(methyl methacrylate) (PMMA, M_w = 120 kDa) at 1300 rpm and then annealed at 100 °C for 40 min. Finally, as gate electrode, Al (80 nm) was vacuum-evaporated on top. All the spin coating processes were conducted in a glove box and OTFTs were measured under ambient conditions with two Keysight B1500A source/measure units. Field-effect mobility in saturation regime was calculated by using the equation: $I_{DS}^{sat} = (\mu C_i W/2L)(V_{GS}-V_T)^2$, in which I_{DS} is the drain-source current, μ is the field-effect mobility, C_i (4.6 nF cm^{-2}) is the capacitance per unit area of the dielectric layer, V_{GS}, V_{DS} and V_T are the gate voltage, drain voltage and threshold voltage, respectively.

Supplementary data

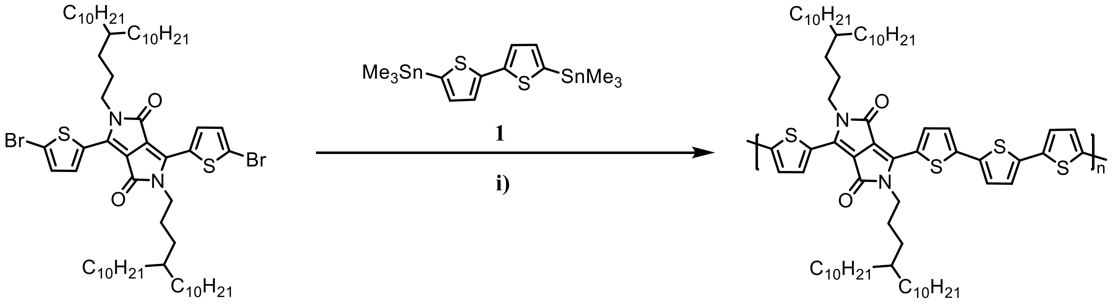

DPPTh-Br

DPPTh-BT

Scheme S1. Molecular structure and synthetic route for **DPPTh-BT**. Reaction condition: i) $Pd_2(dba)_3$, $P(o\text{-}MePh)_3$, toluene, 0.01 mol/L, 110 °C.

The synthesis procedure was according to the literature[1]. GPC: M_n = 187 kDa, $Đ$ = 1.43. Found: C, 72.93; H, 9.28; N, 2.31; S, 11.55. $(C_{74}H_{108}N_6O_2S_2)_n$ requires C, 73.89; H, 9.57; N, 2.46; S, 11.27%.

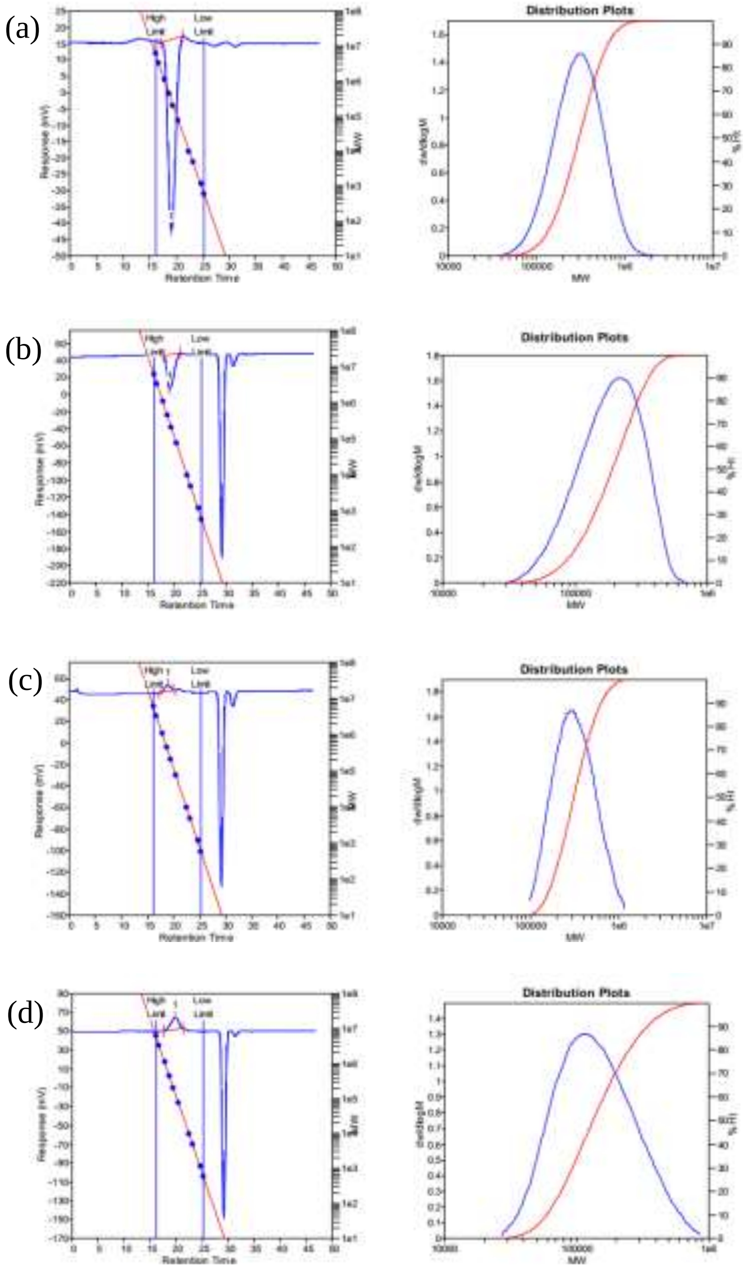

Figure S1. GPC traces of **DPPTh-BT** (a), **DPPTh-BT2CN** (b), **DPPPy-BT2CN** (c) and **2FIID-BT2CN** (d) measured at 150 °C with 1,2,4-trichlorobenzene as the eluent.

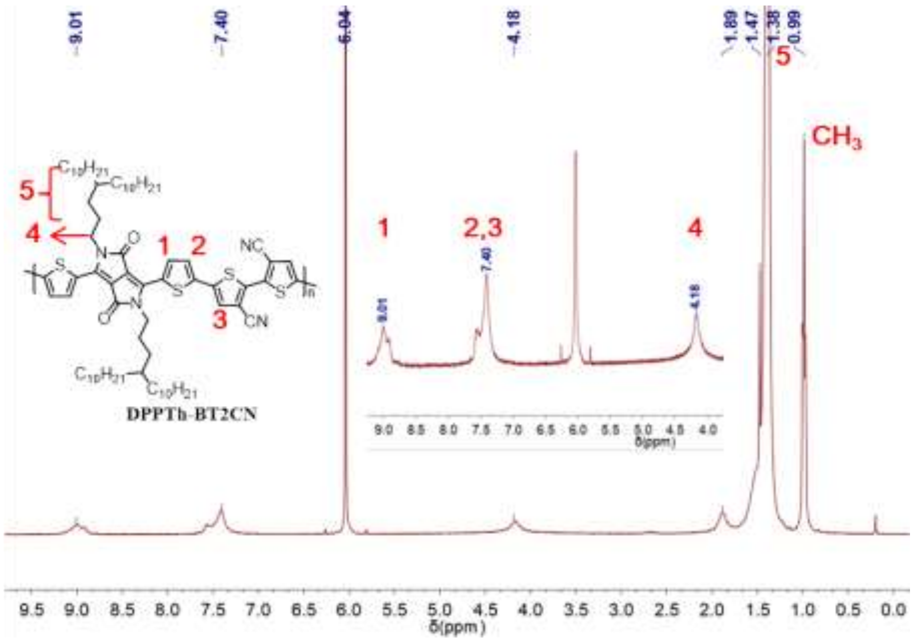

Figure S2. ^{1}H NMR spectrum (400 MHz, $C_2D_2Cl_4$, 120 °C) of **DPPTh-BT2CN**.

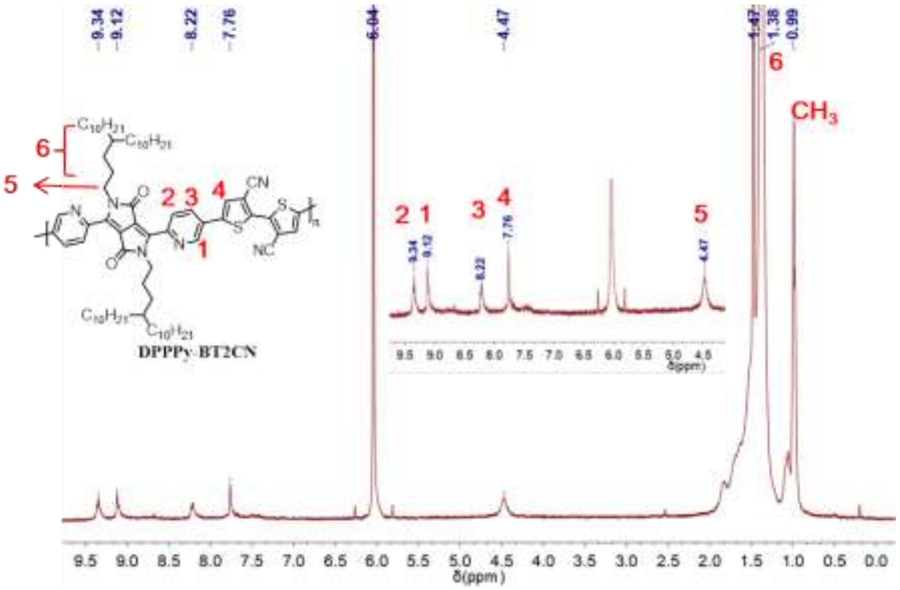

Figure S3. ^{1}H NMR spectrum (400 MHz, $C_2D_2Cl_4$, 120 °C) of **DPPPy-BT2CN**.

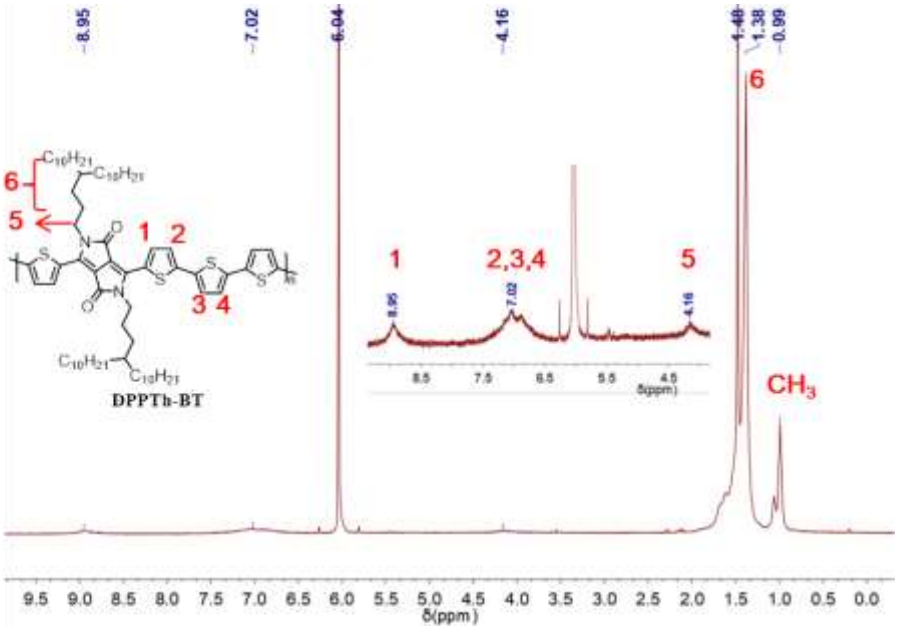

Figure S4. ^{1}H NMR spectrum (400 MHz, $C_2D_2Cl_4$, 120 ^{o}C) of **DPPTh-BT**.

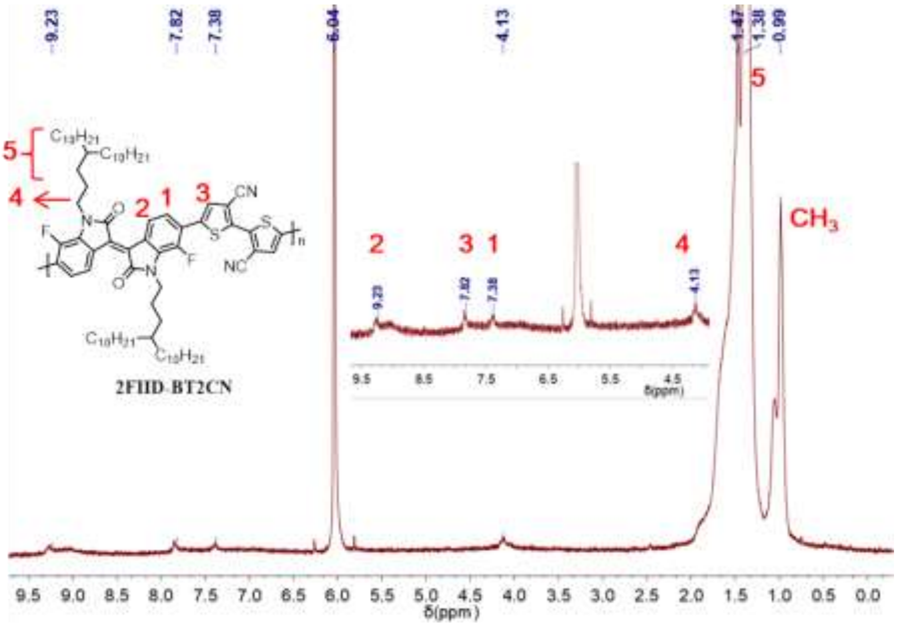

Figure S5. ^{1}H NMR spectrum (400 MHz, $C_2D_2Cl_4$, 120 ^{o}C) of **2FIID-BT2CN**.

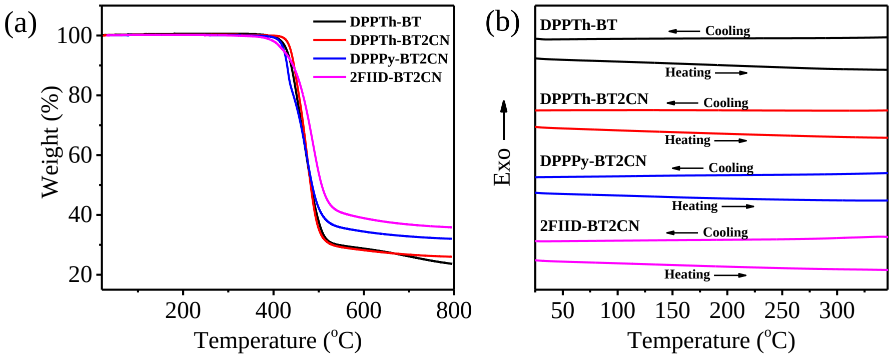

Figure S6. TGA (a) and DSC (b) curves of the polymers measured in N_2 with a heating/cooling rate of 10 °C min^{-1}.

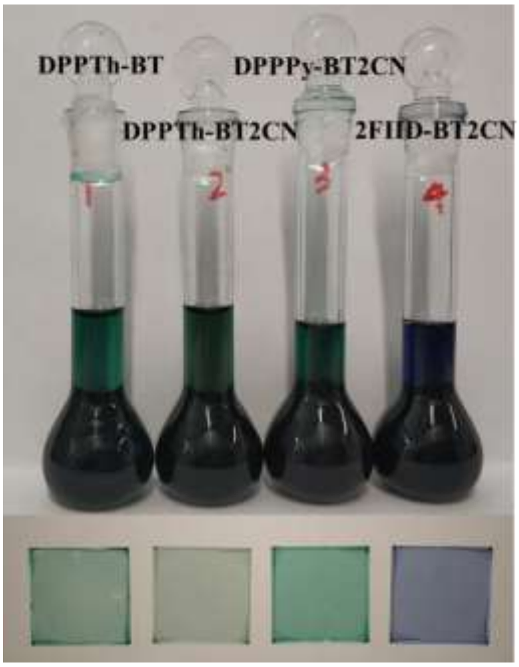

Figure S7. Photographs of the solutions (10^{-4} mol L^{-1} of the repeating units in *o*-DCB) and films of polymers. The thin film was prepared by spin-coating 4 mg mL^{-1} *o*-DCB solution on quartz substrate.

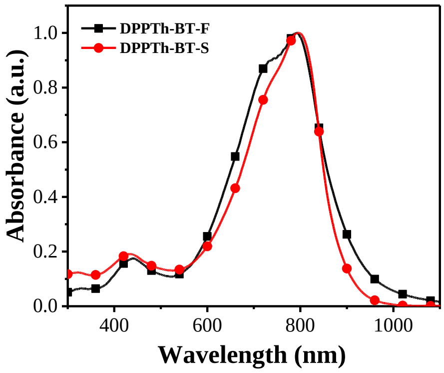

Figure S8. Solution (10^{-5} mol L^{-1} of the repeating units in *o*-DCB) and film UV–vis–NIR absorption spectra of **DPPTh-BT**. The thin film was prepared by spin-coating 4 mg mL^{-1} *o*-DCB solution on quartz substrate.

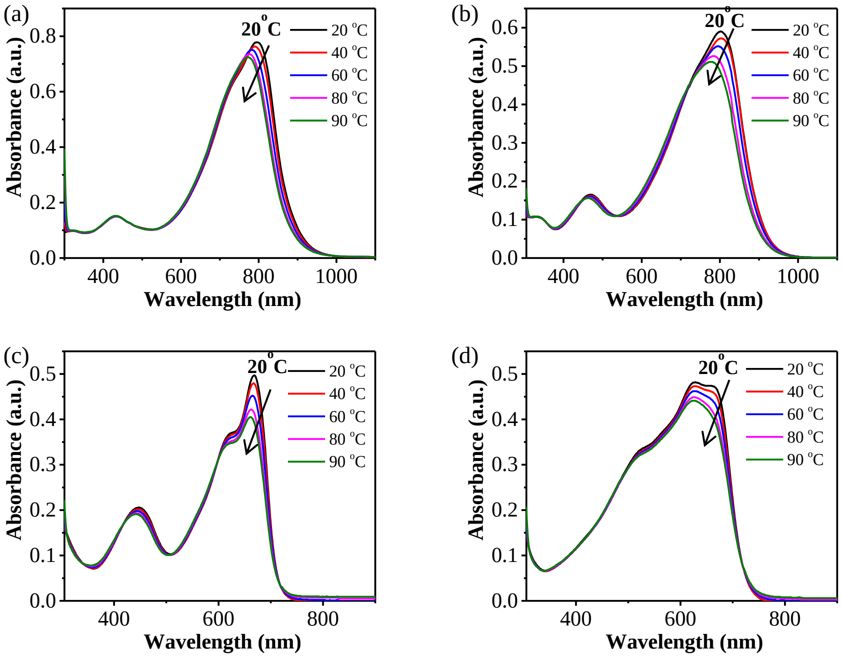

Figure S9. Temperature-dependent solution UV-vis-NIR absorption spectra of **DPPTh-BT** (a), **DPPTh-BT2CN** (b), **DPPPy-BT2CN** (c) and **2FIID-BT2CN** (d) in *o*-DCB (10^{-5} mol L^{-1} of the repeating units).

Table S1. OTFT device performance of **DPPTh-BT2CN**, **DPPPy-BT2CN** and **2FIID-BT2CN** with different annealing temperatures.

Polymer	Annealing	$\mu_{e,max}$ ($\mu_{e,avg}$)	V_T	I_{on}/I_{off}
DPPTh-BT2CN	100 °C	0.20 (0.17)	17~22	10^3~10^4
	150 °C	0.33 (0.27)	30~34	10^3~10^4
	200 °C	0.35 (0.32)	15~25	10^3~10^4
	250 °C	0.31 (0.26)	15~20	10^3
DPPPy-BT2CN	100 °C	0.18 (0.15)	4~8	10^3~10^4
	150 °C	0.25 (0.20)	5~10	10^4~10^5
	200 °C	0.30 (0.25)	1~9	10^4~10^6
	250 °C	0.24 (0.18)	6~10	10^4~10^6
2FIID-BT2CN	100 °C	0.19 (0.16)	5~8	10^3~10^5
	150 °C	0.20 (0.17)	9~15	10^3~10^5
	200 °C	0.25 (0.22)	10~17	10^4~10^5
	250 °C	0.17 (0.15)	10~14	10^3~10^5

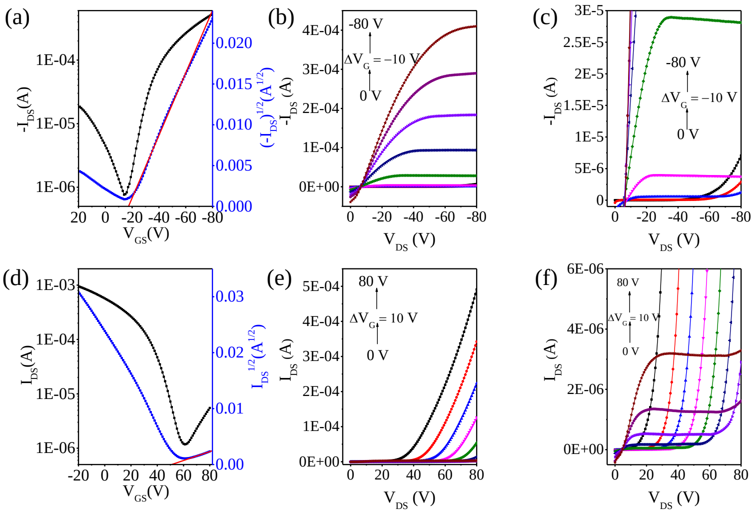

Figure S10. P-type (a, b, c,) and n-type (d, e, f) transfer (a, d) and output (b, e) curves of **DPPTh-BT**; c and f are the enlarged output characteristics (b, e) at low V_{GS}. The polymer films were spin-cast from *o*-DCB solution (4 mg mL^{-1}) and then annealed at 200 °C in N$_2$ for 10 min.

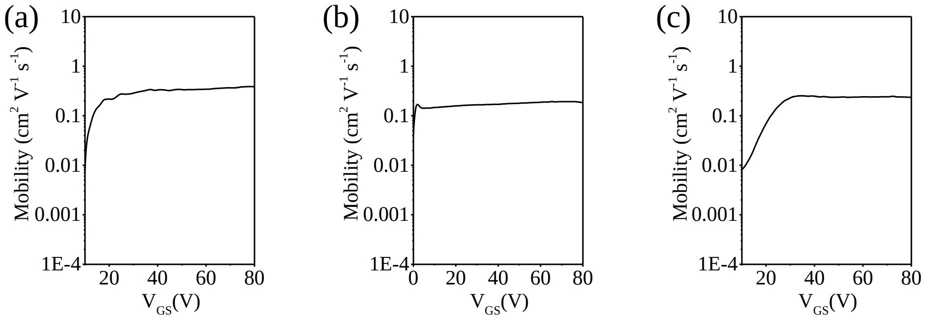

Figure S11. Mobility versus V_{GS} of the devices based on **DPPTh-BT2CN** (a), **DPPPy-BT2CN** (b) and **2FIID-BT2CN** (c) with annealing temperature of 200 °C.

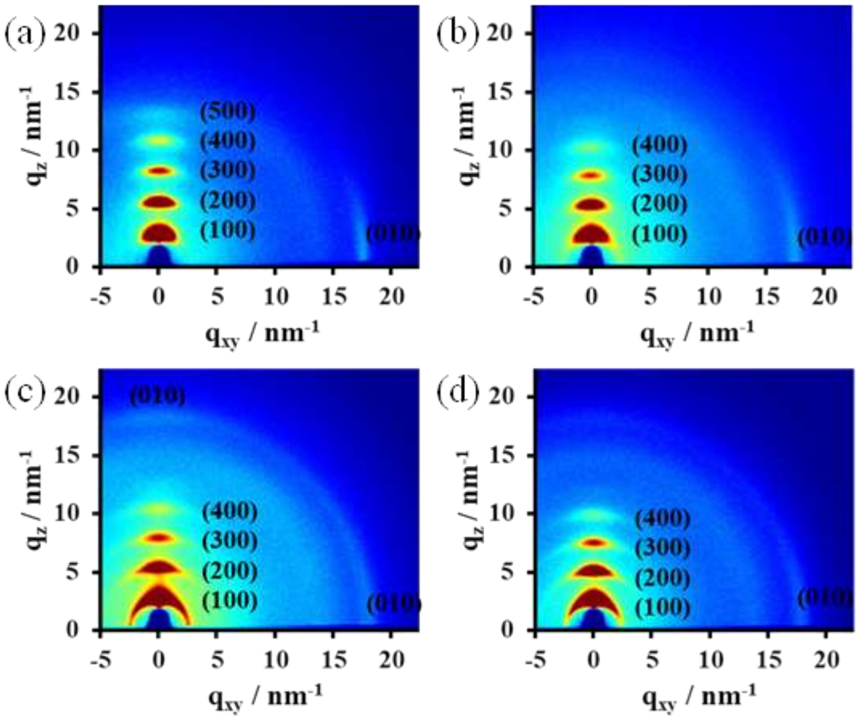

Figure S12. 2D-GIWAXS patterns of the drop-cast films (ca. 1000 nm) of **DPPTh-BT** (a), **DPPTh-BT2CN** (b), **DPPPy-BT2CN** (c) and **2FIID-BT2CN** (d) after being thermally annealed at 200 °C for 10 min.

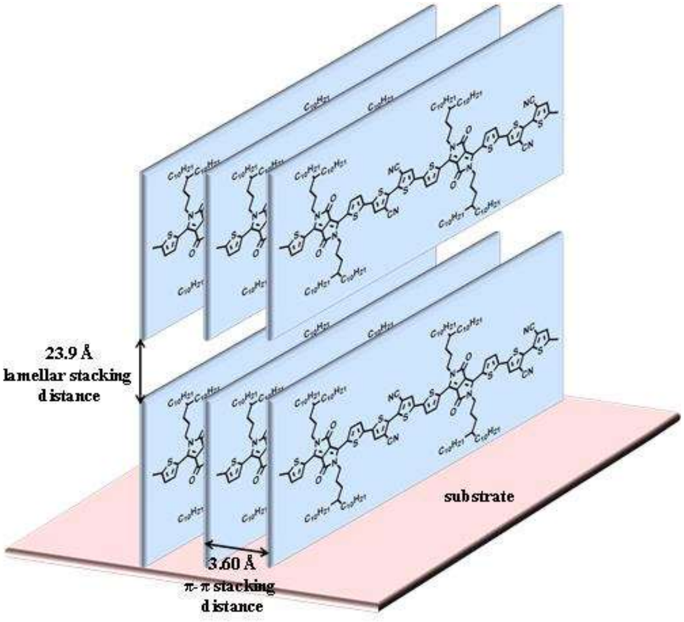

Figure S13. Schematic illustration of edge-on stacking with **DPPTh-BT2CN** as an example.

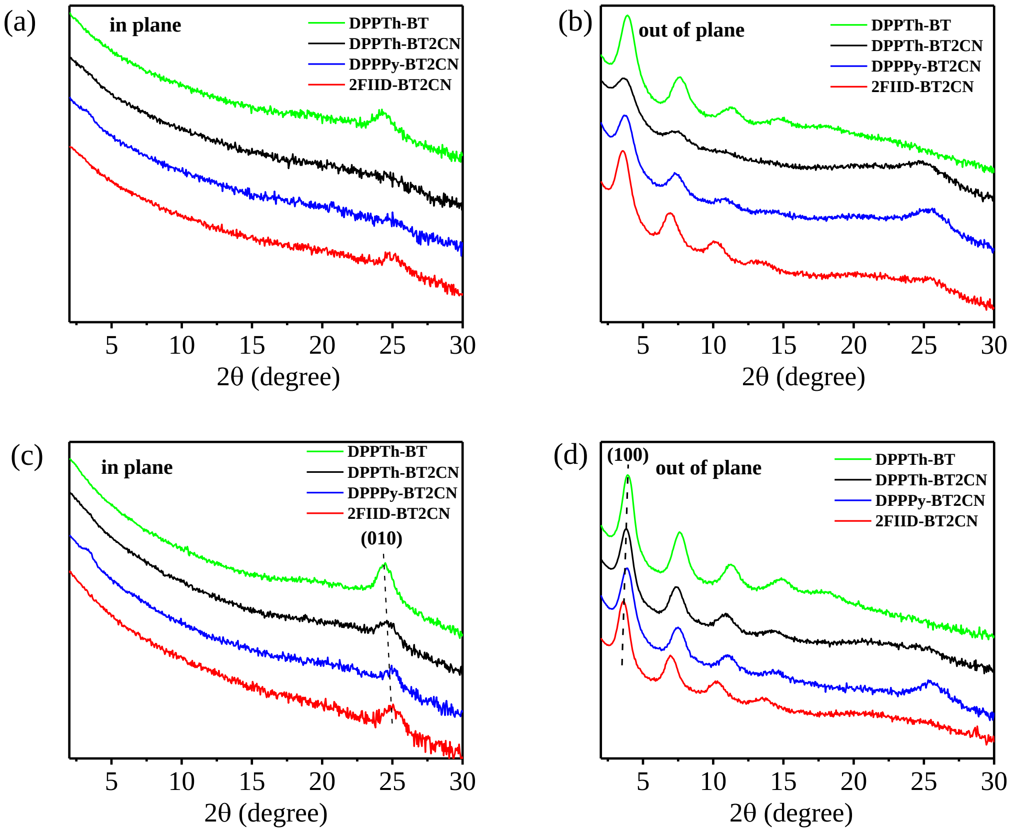

Figure S14. In-plane (a, c) and out-of-plane (b, d) GIWAXS patterns of the spin-coated polymer films (ca. 20 nm) annealed at 100 ^{o}C (a, b) and 200 ^{o}C (c, d) for 10 min.

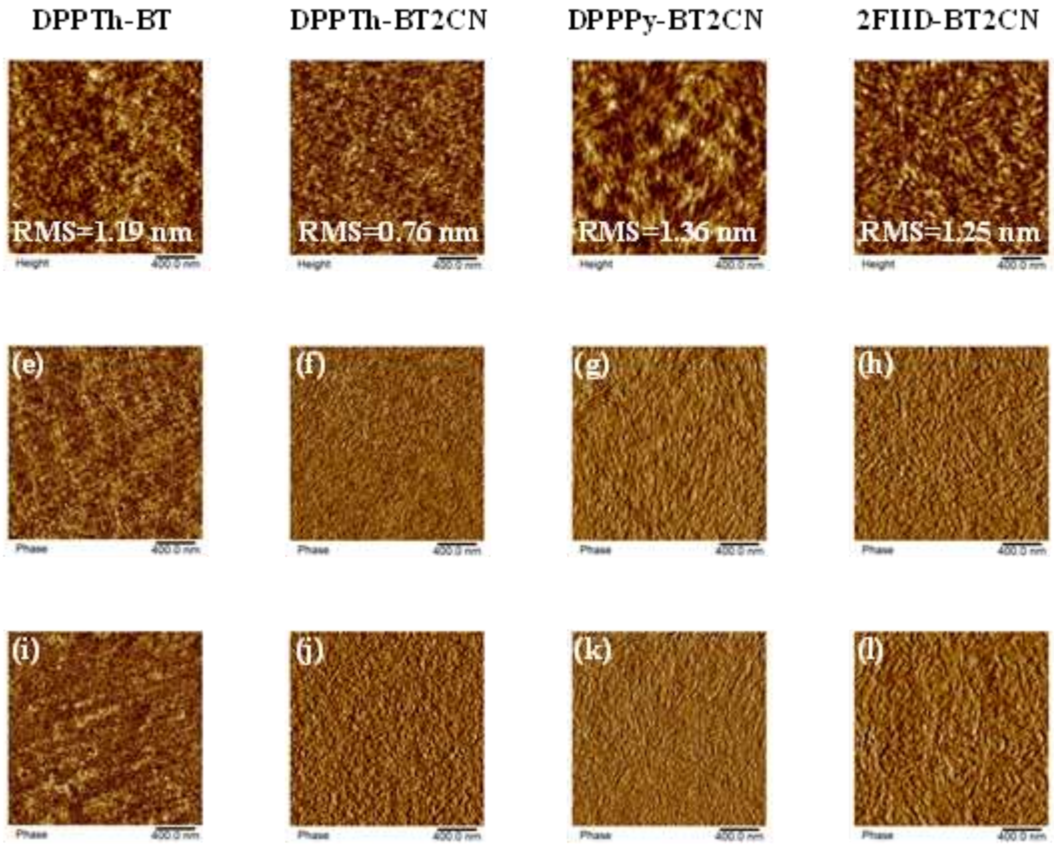

Figure S15. AFM height images (a-d) and phase images (e-l) (2 μm × 2 μm) of the polymer films annealed at 100 ºC (a-h) and 200 ºC (i-l) for 10 min.

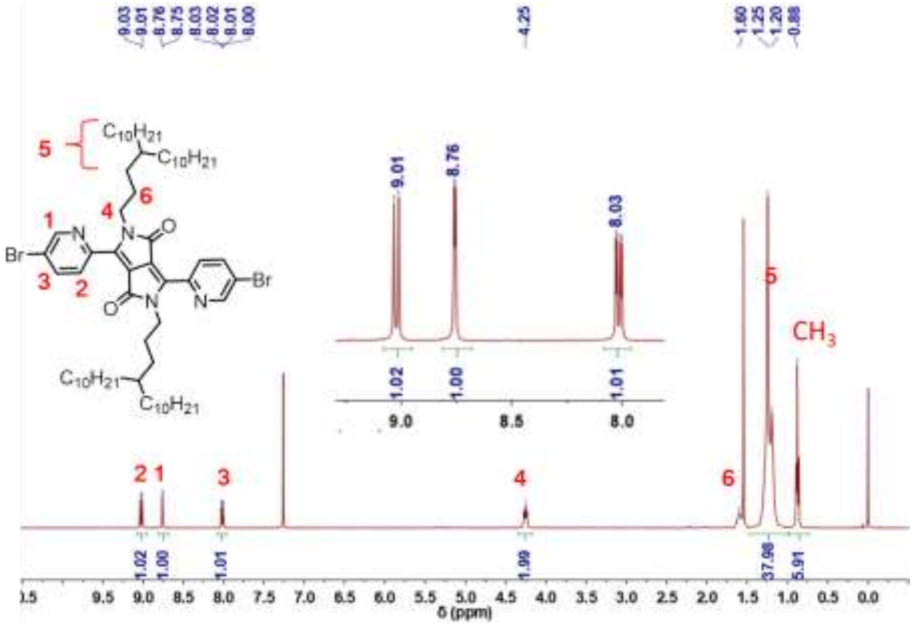

Figure S16. ^{1}H NMR spectrum (400 MHz, $CDCl_3$, 25 °C) of **DPPPy-Br**.

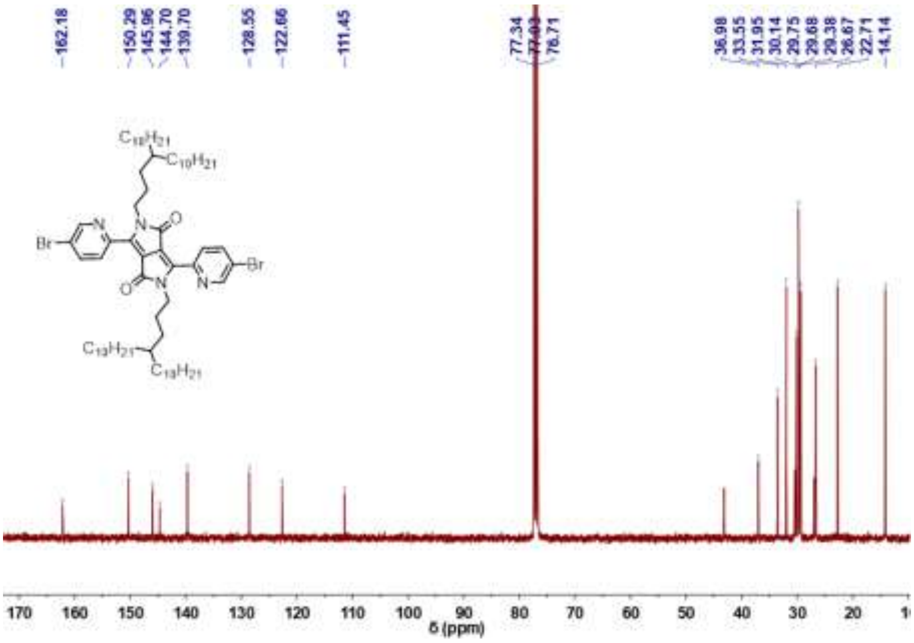

Figure S17. ^{13}C NMR spectrum (100 MHz, $CDCl_3$, 25 °C) of **DPPPy-Br**.

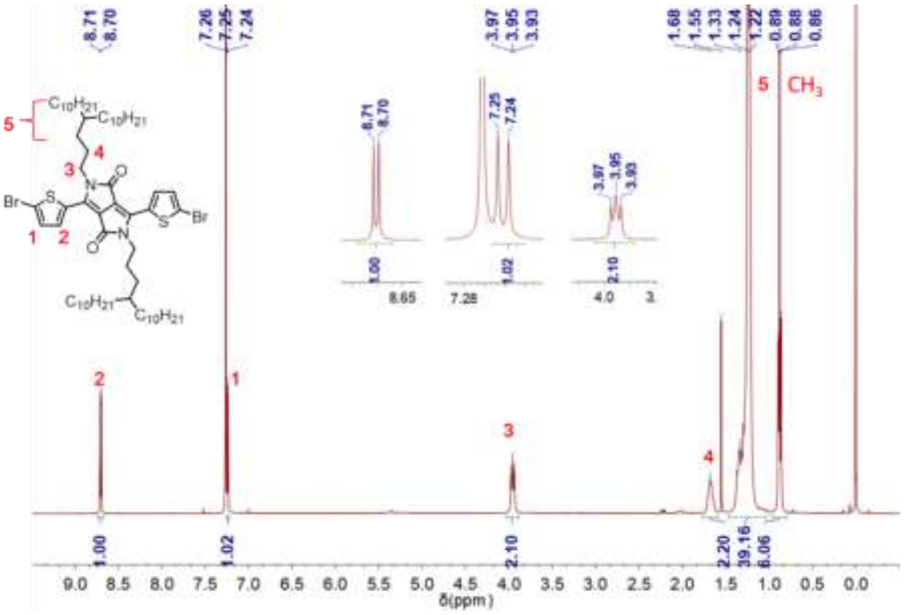

Figure S18. ^{1}H NMR spectrum (400 MHz, CDCl$_3$, 25 °C) of **DPPTh-Br**.

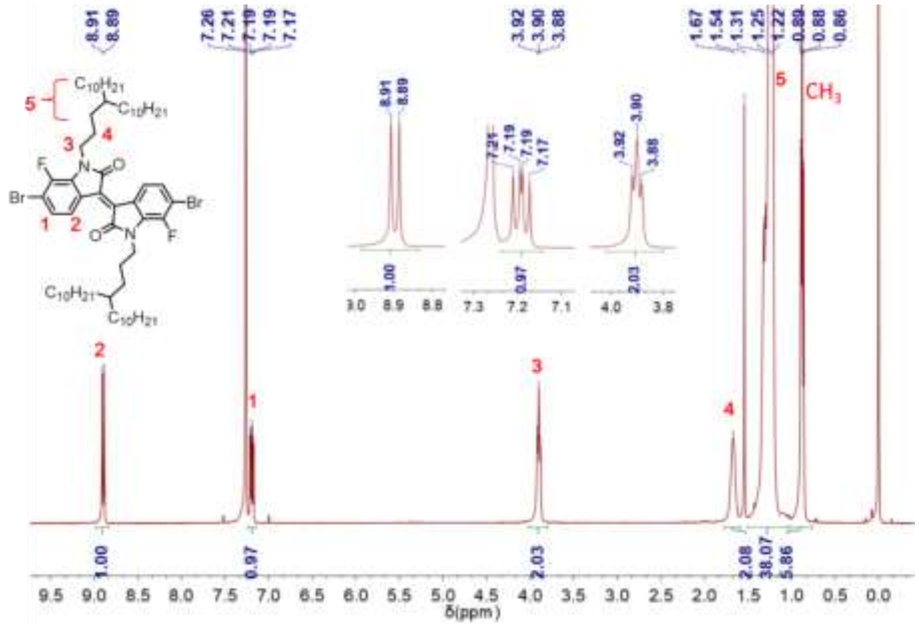

Figure S19. ^{1}H NMR spectrum (400 MHz, CDCl$_3$, 25 °C) of **2FIID-Br**.

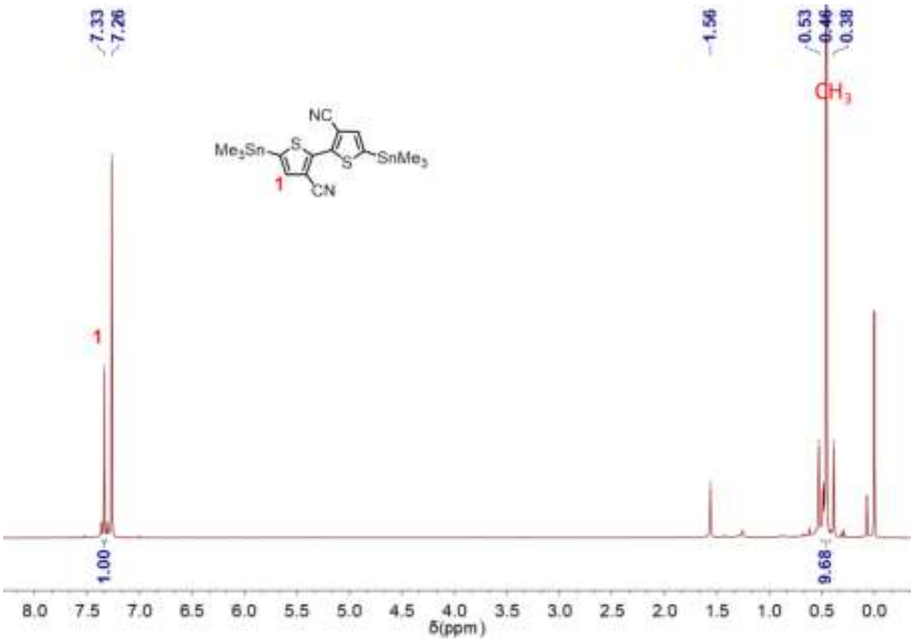

Figure S20. ^{1}H NMR spectrum (400 MHz, CDCl$_3$, 25 ^{o}C) of **1**.

Reference

1 J. Yao, C. Yu, Z. Liu, H. Luo, Y. Yang, G. Zhang and D. Zhang, *J. Am. Chem. Soc.*, 2016, **138**, 173-185.